

Retrieving aerosol optical depth and type in the boundary layer over land and ocean from simultaneous GOME spectrometer and ATSR-2 radiometer measurements

2. Case study application and validation

T. Holzer-Popp, M. Schroedter, and G. Gesell

Deutsches Zentrum für Luft- und Raumfahrt E.V. (DLR), Deutsches Fernerkundungsdatenzentrum (DFD), Oberpfaffenhofen, Germany

Received 28 May 2001; revised 22 July 2001; accepted 5 July 2002; published XX Month 2002.

[1] Intensive research on the distribution of aerosols is being conducted within many international research programs (e.g., Global Energy and Water Cycle Experiment and International Global Atmospheric Chemistry Experiment). Obviously, satellite remote sensing allows for global monitoring; however, operational satellite observation has for a long time been limited to either the oceans or to UV-absorbing aerosols. Therefore a new aerosol retrieval method, Synergetic Aerosol Retrieval (SYNAER), to derive aerosol optical depth and type, both over land and over ocean, was developed (see part 1 of this paper, *Holzer-Popp et al.* [2002]). First, case studies showing its application and a validation using ground-based and airborne measurements are presented. They show a good agreement with better than 0.1 in boundary layer aerosol optical thickness at 550 nm and indicate a detection of the correct aerosol type in most cases. Restrictions for the detection of aerosol type appear over bright surfaces and in areas with an aerosol optical depth less than 0.1 due to a low aerosol sensitivity in these situations. The method has been developed for the future operational use of similar sensor pairs Scanning Imaging Absorption Spectrometer for Atmospheric Cartography (SCIAMACHY)/Advanced Along Track Scanning Radiometer (AATSR) and Global Ozone Monitoring Experiment 2 (GOME-2)/Advanced Very High Resolution Radiometer (AVHRR). Thus SYNAER holds the potential to extract a 25-year-long climatological data set (1995–2020) from ERS-2, Envisat, and METOP. *INDEX TERMS*: 0305 Atmospheric Composition and Structure: Aerosols and particles (0345, 4801); 0345 Atmospheric Composition and Structure: Pollution—urban and regional (0305); 0365 Atmospheric Composition and Structure: Troposphere—composition and chemistry; 1640 Global Change: Remote sensing; 1694 Global Change: Instruments and techniques; *KEYWORDS*: aerosol retrieval, remote sensing

Citation: Holzer-Popp, T., M. Schroedter, and G. Gesell, Retrieving aerosol optical depth and type in the boundary layer over land and ocean from simultaneous GOME spectrometer and ATSR-2 radiometer measurements, 2, Case study application and validation, *J. Geophys. Res.*, 107(0), XXXX, doi:10.1029/2002JD002777, 2002.

1. Introduction

[2] Aerosols affect climate directly by interaction with solar and terrestrial radiation and indirectly by their effect on cloud microphysics, albedo and precipitation as cloud condensation nuclei [*Intergovernmental Panel on Climate Change (IPCC)*, 1992, 1995]. Tropospheric aerosol forcing is comparable to global net cloud forcing of approximately -1 Wm^{-2} [*Charlson and Heintzenberg*, 1995]. However, on regional scales the mean direct radiative forcing by aerosols can be as large as -10 Wm^{-2} as was reported for mineral dust over ocean [*Teegen et al.*, 1996]. Anthropogenic changes of the global aerosol distribution may enhance greenhouse warming [*Jacobson*, 2001]. The net

effect of aerosol radiative forcing depends strongly upon the aerosol composition. Current understanding of aerosol impact is beginning to extend beyond the sulfate aerosol that has been used as the sole aerosol component in climate models up to now. It is recognized that smoke aerosol and mineral dust are equally important and may regionally enhance greenhouse warming [*Andreae*, 2001]. For a review of aerosol impact on climate, see *Charlson and Heintzenberg* [1995].

[3] Due to the aerosol variability and its influence on radiative transfer, a quantitative analysis of land and ocean surface observations is often hampered by remote sensing without atmospheric correction of the aerosol impact [*Ver-mote et al.*, 1997]. Additional upcoming applications for aerosol measurements from satellites include: health monitoring of particulate matter, accurate assessment of surface UV irradiance and the derivation of direct and diffuse

surface irradiance for solar energy applications, and calculation of the photosynthetically active radiation which determines carbon uptake in vegetation.

[4] Currently, several aerosol monitoring schemes using earth observation are available, but each of them has deficiencies in delivering operationally aerosol optical thickness and type over land and ocean. Therefore a new aerosol retrieval method SYNAER (Synergetic Aerosol Retrieval) was developed, which delivers boundary layer optical thickness (BLAOT) and the aerosol type both over land and ocean, as outlined in part 1 of this paper [Holzer-Popp *et al.*, 2002].

[5] It uses simultaneous data of the Along Track Scanning Radiometer (ATSR-2) and the spectrometer Global Ozone Monitoring Experiment (GOME), both onboard the ERS-2 satellite. ATSR-2 measures earth reflected radiances in 5 spectral bands centered at 0.55, 0.67, 0.87, 1.6, 3.7 μm with bandwidths of 25 to 66 nm and brightness temperatures in 2 thermal channels at 11 and 12 μm . All observations are taken under two viewing angles (nadir and 52° forward) with a ground resolution of approximately 1.1 km^2 . GOME observes near-nadir reflection from the Earth in the range from 240 to 790 nm with a spectral resolution of 0.2 nm to 0.4 nm and a pixel size of either $320 \times 40 \text{ km}^2$ or $80 \times 40 \text{ km}^2$.

[6] Especially for validation of new satellite instruments, the ground-based radiometer network AERONET has been established [Holben *et al.*, 1998, 2001]. From sun and sky scanning measurements at 440, 670, 870, 940, and 1020 nm, aerosol optical thickness, size distribution and water vapor column are derived and can easily be obtained via the World Wide Web (<http://aeronet.gsfc.nasa.gov:8080>).

[7] In part 1 [Holzer-Popp *et al.*, 2002] a detailed description of the methodology and its underlying assumptions is given. This part II contains a short overview over SYNAER in section 2. In sections 3 and 4 a first application and a case study validation based on AERONET measurements and LIDAR measurements from one airborne campaign are presented. Section 5 summarizes and discusses the validation results and the application potential of this method.

2. Retrieval Method

[8] Aerosol parameters are retrieved with the new method SYNAER (Synergetic Aerosol Retrieval) [Popp *et al.*, 1997; Holzer-Popp *et al.*, 1998, 2000a, 2000b, 2002; Holzer-Popp and Schroedter, 1999] from a combination of simultaneous ATSR-2 and GOME measurements. The high spectral resolution of GOME ideally supplements the high spatial resolution of ATSR-2. In this method cloud detection is first performed for all ATSR-2 pixels. Second, dark fields (dark vegetation, water bodies) are selected automatically from the data itself in the 1.6 μm and 3.7 μm channels and from the Normalized Difference Vegetation Index (NDVI) calculated with the 670 and 870 nm channels. Then boundary layer aerosol optical thickness (BLAOT) values at 670 nm (over land) and 870 nm (over ocean) are derived for these dark ATSR-2 nadir pixels for which the surface albedo can be estimated with good accuracy. BLAOT values over the irregularly distributed dark fields are interpolated to all cloud free ATSR-2 pixels with a distance-weighting scheme. Using the atmospheric correction scheme EXACT [Popp, 1995],

which has been validated using Landsat-TM and NOAA-AVHRR data, the surface albedo values for the 3 wavelengths 560 nm, 670 nm and 870 nm are obtained for all cloud free pixels. The ATSR-2 derived parameters are co-registered to GOME pixels and interpolated spatially. BLAOT and surface albedo calculation is repeated for 40 different aerosol mixtures that are defined by external mixing of six basic aerosol components. Using the ATSR-2 calculated values of optical thickness and surface albedo, GOME surface and consecutively top-of-the-atmosphere spectra for the same set of different mixtures are simulated at 10 selected wavelengths. The measured GOME spectra are corrected for cloud and ozone influence. A least square fit of the simulated to the measured GOME spectrum selects the most plausible type of aerosol and its corresponding BLAOT value at the reference wavelength of 550 nm in a GOME pixel. Finally, a quality control and an ambiguity test are applied by comparing the fit error with deviations between different mixtures.

3. Example Result

[9] Figure 1 shows the SYNAER results for a 3-day data set of GOME and ATSR-2 over Europe on 1–3 September 1995. Retrieved boundary layer aerosol optical thickness at 550 nm (BLAOT550) is seen in the upper part, and the retrieved percentage contributions of six basic aerosol components (depicted as percentage of the pixel area) are shown in the bottom. Cloud-covered GOME pixels (above 50% fraction) are excluded, as are pixels that failed the quality control. The ambiguity test was not applied here. In the case of the aerosol type map this ambiguity test would reject a large number of pixels when simulated spectra of different types accurately fit the measured spectrum but differ too little to decide which is the best in the limit of the observation accuracy. But it seems that despite this, the retrieved result is plausible. Therefore the ambiguity test shall be further investigated with larger amounts of validation observations.

[10] It can be seen that the retrieved boundary layer aerosol optical thickness shows several well-known features: The highest BLAOT values occur in the Po basin and in some industrial or densely populated areas in Germany, France, Spain and Greece and low values are found over oceans, in high mountain areas and in Russia. At land/ocean boundaries BLAOT values show no significant steps. The selected aerosol mixtures show the water-soluble aerosol component as a general background (which is due to the definition of the 40 mixtures). Soot contributions can be seen especially in Central Europe and in Russia. Transported minerals occur over the western Mediterranean and in Turkey. Sea salt can be seen over oceans and in some locations inland and occurs only in the accumulation mode (the coarse mode has a rather short lifetime). It seems that the retrieval prefers soot and transported minerals to the larger insoluble particles (all of which are significantly absorbing), which could be due to the fact that GOME reflectances are 2–4% lower than corresponding ATSR-2 values and thus the stronger absorbing and less scattering smaller particles yield better simulations. Evidently some individual pixel results are doubtful. The type retrieval should be taken cautiously in pixels with low BLAOT

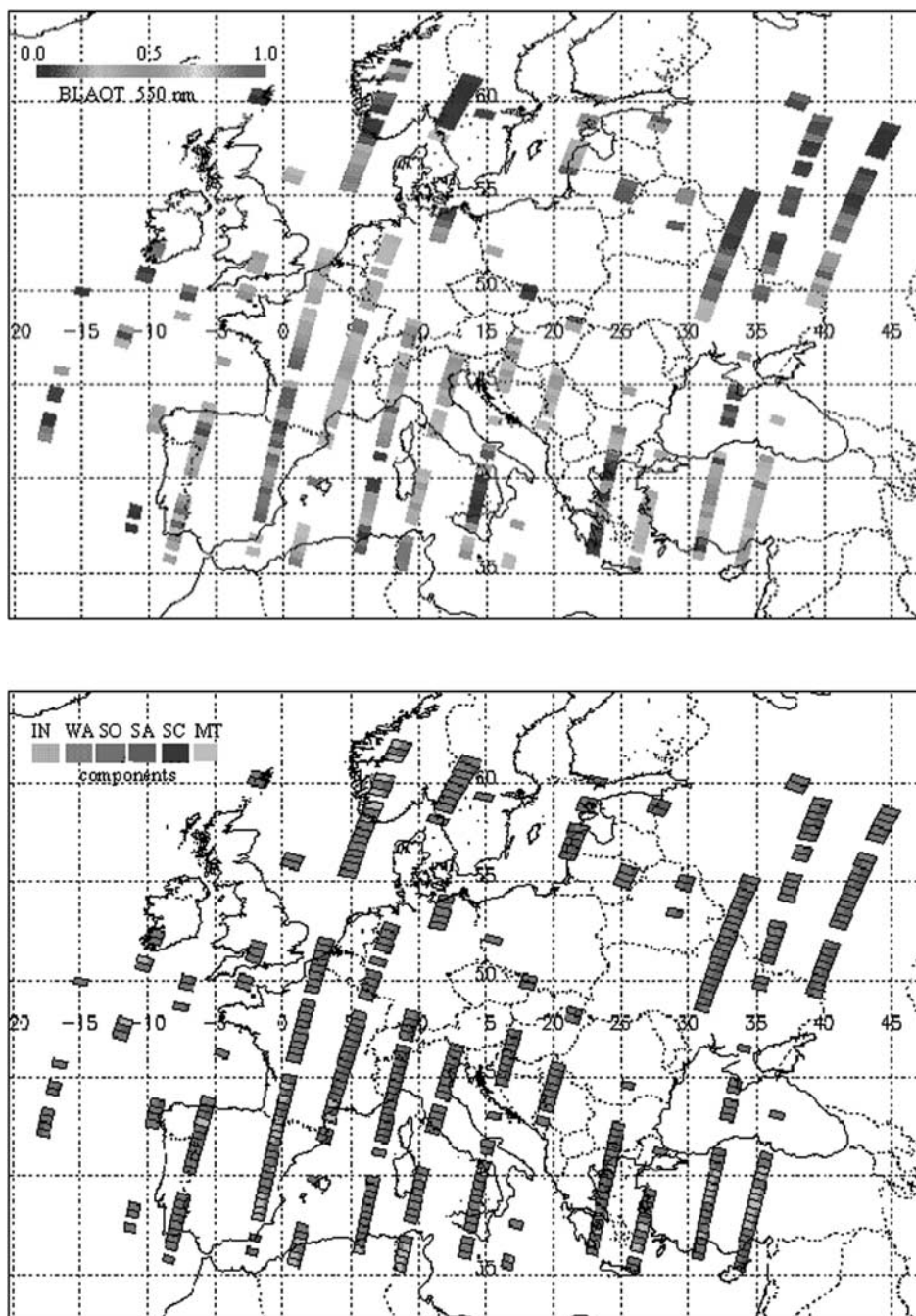


Figure 1. SYNAER 3-day map over Europe for 1–3 September 1995. Retrieved boundary layer optical thickness at 550 nm is shown in the upper part ranging from 0.03 to 0.55. Retrieved percentage contributions of six basic aerosol components (depicted as percentage of the pixel area) are shown in the bottom (IN, insoluble; WA, water-soluble; SO, soot; SA, sea salt accumulation mode; SC, sea salt coarse mode; MT, mineral transported). Cloud-covered GOME pixels above 50% cloud fraction are excluded. Pixels with large fit errors were excluded from both maps by the quality check. The ambiguity test was not applied. See color version of this figure at back of this issue.

(e.g., in Scandinavia) due to the low signal sensitivity in these cases. Also fine differentiations (of 5% in large particle components, and 10% in the others) cannot be separated. However, for getting an overview of significant occurrences of different aerosol mixtures in larger areas of $5^\circ \times 5^\circ$ grid cells the type retrieval map looks promising.

[11] High spatial resolution of aerosol optical thickness is needed for applications such as air quality studies. Using the GOME-retrieved aerosol type in each ATSR-2 frame of 512×512 pixels, a high-resolution aerosol map from the 1–3 September 1995 data set was derived [Holzer-Popp *et al.*, 2000a] and is shown in Figure 2. Here, totally and partly

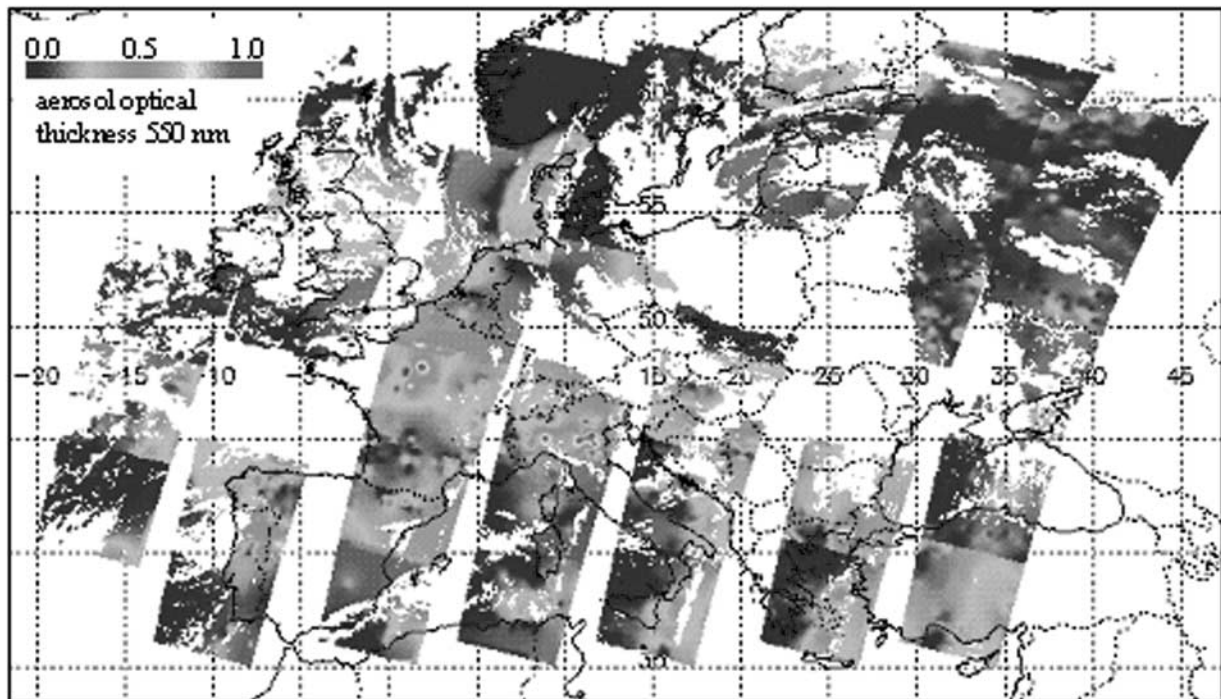


Figure 2. High-resolution aerosol map over Europe. Aerosol optical thickness at 550 nm for all daytime ATSR-2 frames acquired over Europe during the period 1–3 September 1995 (corresponding to the simultaneously measured GOME pixels in Figure 1) with a 1 km horizontal resolution. This result was achieved as post-processing of the SYNAER result based on GOME and ATSR-2 data shown in Figure 1. Cloud-covered pixels are left blank. Gaps between the 512 km swath of the ATSR-2 instrument are also left blank. Aerosol optical thickness ranges from 0.01 to 0.99. See color version of this figure at back of this issue.

cloudy ATSR-2 pixels are masked in white. Interesting features are local maxima of aerosol optical thickness in urban areas such as Paris, northern Italy, west of Madrid, and near Thessaloniki. Lower values over the Alps and the Pyrenees occur as expected. Around Denmark a band of higher optical thickness occurs, however, that might be due to cloud detection errors and this will require further investigation. As a weakness, stepwise transitions between ATSR-2 frames can be seen. This is due to two reasons. First, the exploited GOME scan mode (of the commissioning phase) has a swath width of 240 km and does not cover the whole ATSR-2 frame. Therefore the most frequent aerosol type of all GOME pixels inside an ATSR-2 frame was chosen. Using this frame-specific aerosol type AOT was calculated for each frame separately. Second, the dark field selection is handled in a framewise manner ($512 \times 512 \text{ km}^2$) and therefore border effects might contribute to these edges. In the future application of SYNAER to SCIAMACHY and AATSR, this difficulty will be overcome because the measurements from both sensors will cover the same swath width of 512 km and AATSR data will be delivered orbitwise.

4. Case Study Validation

[12] For the first case studies, ground-based measurements taken by the AERONET stations were used. The

objective of AERONET is to monitor aerosols by ground-based measurements and it was especially designed for the validation needed for satellites such as ENVISAT, TERRA and ADEOS-2. The measurements are processed in near real-time, archived and made available to the public by NASA <http://aeronet.gsfc.nasa.gov:8080>. AERONET provides spectral aerosol optical thickness, aerosol size distributions and water vapor column taken since 1993 using automatic sun-sky scanning spectral radiometers at approximately 50 ground stations worldwide.

[13] So far, about 2500 GOME pixels were analyzed with SYNAER, but only 66 pixels include ground stations inside the pixel boundaries. Criteria for validation pixels are (1) cloud free ground-based measurements, (2) less than 50% cloud coverage inside the GOME pixel, and (3) a maximum of 15 minutes difference between ground measurement and satellite overpass. These criteria left 29 pixels with corresponding ground measurements of spectral aerosol optical thickness values so far. Ground measurements of size distributions are not available for these pixels.

[14] From these 29 pixels another 15 cases were excluded for the following reasons: altitudes above 1.5 km (6 cases), noisy GOME spectra (3 cases), or very bright surfaces (2 cases). Another exclusion was made when dark fields were situated in valleys but the sun photometer station was positioned at an elevated location. In 3 cases the AERONET station was at the edge of a turbid area that covered much of

Table 1. Validation Pixels and Results^a

Date and UTC Time	Latitude and Longitude	Altitude, m	Orbit Number	Pixel Number	Location	Country	Cloud Fraction	Retrieved AOT550	Aerosol Type
15/08/97 09:39	45:18N 12:30E	10	12129	818	Venice	Italy	5.4%	0.45	heavy pollution
15/11/97 10:24	45:48N 08:37E	235	13446	419	Ispra	Italy	6.1%	0.12	heavy pollution, humid
14/07/98 14:28	16:00S 62:01W	500	16898	1596	Concepcion	Bolivia	0.0%	0.12	biomass burning
14/7/98 14:24	14:33S 60:55W	225	16898	1579	Los Fieros	Bolivia	0.0%	0.08	heavy pollution, humid
14/7/98 13:54	17:15S 63:14W	225	16898	1613	Santa Cruz	Bolivia	0.0%	0.12	polluted maritime
24/7/98 17:06	36:36N 97:24W	315	17043	986	Cart Site	USA	35.0%	0.35	continental
15/8/98 10:39	49:18N 7:45E	400	17354	767	Pfälzer Wald	Germany	0.0%	0.19	heavy pollution
24/8/98 16:10	39:01N 78:50W	50	17486	854	GSFC	USA	0.0%	0.60	heavy pollution
4/10/98 17:50	55:47N 97:50W	218	18074	474	Thompson	Canada	29.0%	0.17	heavy pollution, humid
25/10/98 8:42	15:15S 23:09E	1107	18369	1174	Mongu	Zambia	0.0%	0.28	desert outbreak
4/4/99 16:07	37:55N 75:29W	10	20678	802	Wallops	USA	7.0%	0.40	polluted maritime
4/6/99 10:50	12:11N 1:23W	290	21548	1281	Ouagadougou	Obervolta	5.0%	0.65	desert outbreak, humid
4/6/99 17:13	36:36N 97:24W	315	21552	1010	Cart Site	USA	0.0%	0.20	desert outbreak
4/6/99 18:46	46:29N 116:59W	824	21553	893	Rimrock	USA	12.0%	0.07	polluted watersoluble
14/8/99 18:24	53:55N 106:00W	550	22569	724	Wasquesiu	Canada	4.0%	0.05	polluted watersoluble

^aCharacteristics of the validation cases (14 from AERONET, 1 airborne), showing the location and time of observation together with numbers of exploited GOME pixels. The last three columns give the results: cloud fraction, retrieved AOT at 550 nm, and retrieved aerosol mixture. AERONET data were acquired through the AERONET website of NASA-GSFC (<http://aeronet.gsfc.nasa.gov:8080>) courtesy of B. Holben/NASA-GSFC.

the GOME pixel spoiling the comparison of a GOME pixel averaged SYNAER result to the point measurement of AERONET. The validation was conducted with the remaining 14 cases. Here, SYNAER was driven by dark fields over land. The specifications of the 14 test cases are given in Table 1. All GOME pixels have a size of $80 \times 40 \text{ km}^2$ (except orbit 21548 with large GOME pixels of $320 \times 40 \text{ km}^2$). Figure 3 shows the retrieved AOT values at 6 wave-

lengths (340, 380, 440, 500, 670, and 870 nm) against AERONET measurements. A good agreement with RMS errors of 0.104 at 440 nm and 0.067 at 670 nm for the AOT values can be seen. The spectral agreement of retrieved AOT values at all 6 wavelengths indicates that the retrieval of aerosol mixtures works well. Furthermore, the selected aerosol mixture as listed in the last column of Table 1 is plausible except for the two pixels at Santa Cruz/Bolivia

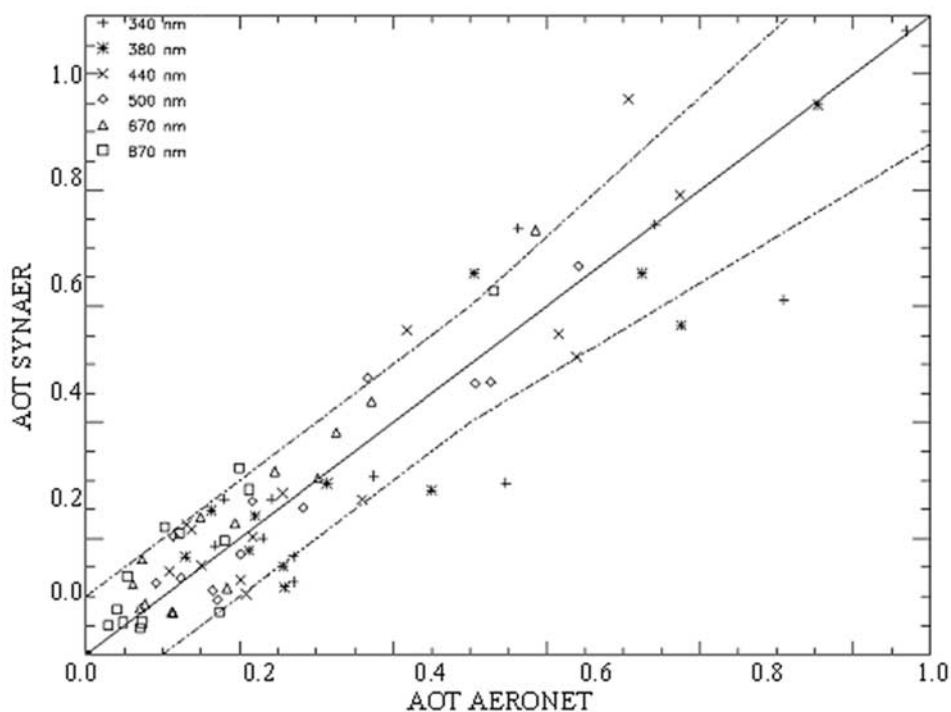


Figure 3. First validation results. Comparison of spectral aerosol optical thickness (AOT) retrieved with SYNAER to AOT measured by 14 AERONET ground stations and 1 airborne observation. Different wavelengths are marked with different symbols; for some stations, not all wavelengths are available. AERONET data were acquired through the AERONET website of NASA-GSFC (<http://aeronet.gsfc.nasa.gov:8080>). The solid line indicates accurate agreement; the dashed lines show an error range of ± 0.1 or $\pm 20\%$ for higher AOT values.

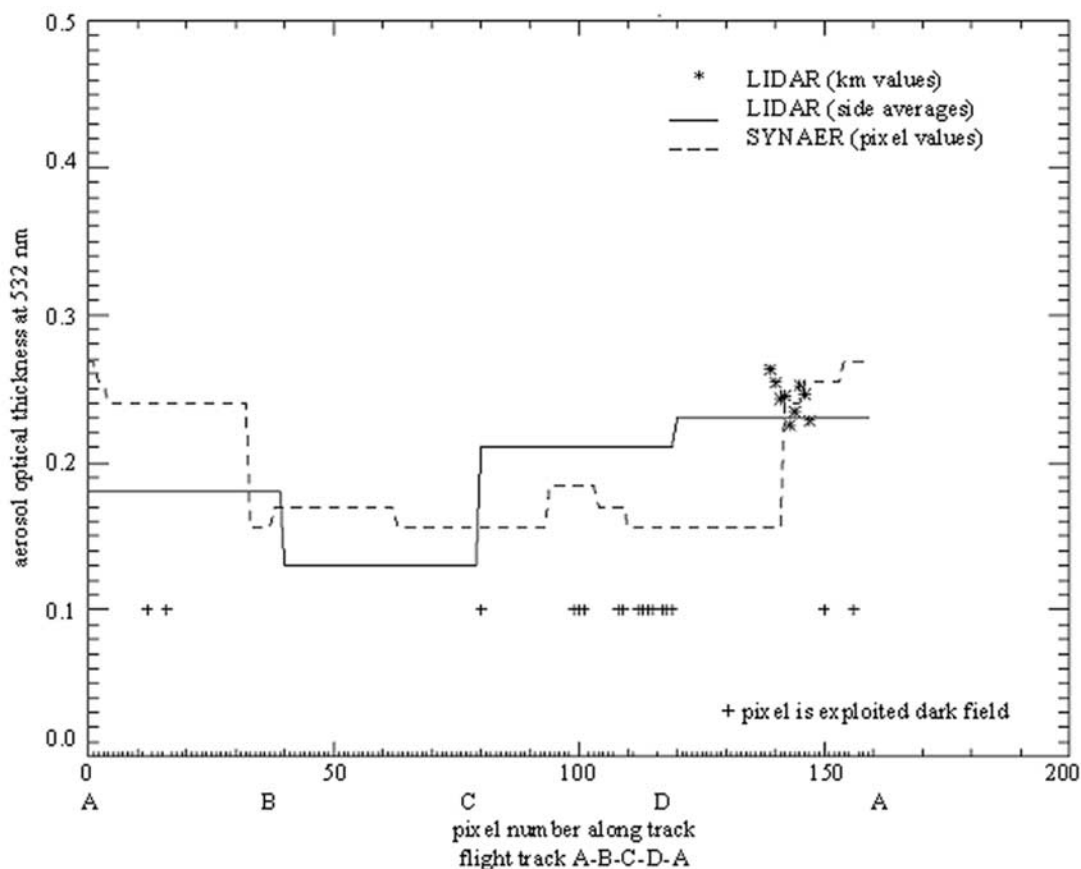


Figure 4. Comparison of LIDAR measurements to SYNAER results. For the airborne measurements, LIDAR and SYNAER aerosol optical thickness (AOT) values at 532 nm along the flight path are compared. Lines give AOT values along the path on a 1-km grid (SYNAER) and averaged values (LIDAR) over the 4 sides of the flown rectangular pattern. Individual 1-km LIDAR averages are indicated (asterisks, at the right side of the graph). Exploited dark fields in SYNAER along the flight track are indicated with a plus sign

and Mongu/Zambia. In the case of Santa Cruz, a maritime aerosol mixture is not plausible for a land-locked site, but due to the low aerosol optical thickness value the aerosol type sensitivity is small. In the case of Mongu the dominant aerosol source for that time of the year is biomass burning; desert dust may occur but at other times of the year. In this case (with significant aerosol loading) a close look at the 6 spectral optical thickness values in the validation plot reveals an almost horizontal line, which indicates an incorrect detection of the aerosol type. The GOME surface spectrum shows a bright ground with surface albedo values linearly increasing from 0.05 at 400 nm to 0.13 at 700 nm and even all dark fields selected in the GOME pixel belonging to dark field class 3 and having a surface albedo brighter than 0.06 at 670 nm. This first ground-based validation comprises data from 4 continents (the Americas, Europe, Africa) in several climate zones (latitudes 17 South to 56 North) distributed over 2 years except the winter season with solar elevations ranging from 25 to 60 degrees. The cloud fraction inside the GOME pixels ranged up to 35%.

[15] A second case study was conducted with airborne measurements. During an ERS-2 overpass airborne LIDAR data and particle counter measurements at different heights

were collected (upper flight level at 11277m completed at 10:34 UTC) which corresponds to the eastern half of GOME pixel number 767 in orbit 17354 on 15 August 1998 at 10:44 UTC (the flight track is shown in Figure 5 of part 1 of this paper). Due to some cirrus clouds these data could not be exploited in terms of vertical profiles or particle characteristics. Only the aerosol optical thickness could be retrieved from the LIDAR measurements. These results (at the 2 LIDAR wavelengths at 532 and 1064 nm) are included as "Pfälzer Wald" in Table 1 and Figure 3. A very good agreement was found with a GOME pixel averaged AOT at 532 nm of 0.189 and a LIDAR averaged result (which corresponds to the right half of the GOME pixel only) of 0.187. To investigate the capabilities and limitations of the dark field approach, the spatial variability inside a GOME pixel (along the flight track) was compared to LIDAR derived aerosol optical thickness and the SYNAER results from the interpolated AOT mask (Figure 4). SYNAER results are given as a dashed line. LIDAR measurements were exploited as averages over each flight track (solid line) and some individual measurements (asterisks) are also shown at the right side (showing the 1-km variability). 1-km LIDAR measurements could only be exploited if no cirrus contamination occurred. A good

agreement within 0.05 can be found, especially at the step at the right where individual lidar measurements were exploited and are quite well represented in both data sets. The limitation due to the availability of dark fields is seen at the left part of the flight track A-B (location of dark fields along the flight track is indicated as plus sign in the graph) where the density of dark fields along the path is too low.

5. Discussion and Conclusions

[16] SYNAER, a new synergetic retrieval method for aerosol optical thickness and type in the boundary layer over land and ocean from GOME and ATSR-2 data, was developed (see part 1 [Holzer and Popp, 2002]) and applied. It was demonstrated that the combination of a radiometer and a spectrometer can be used to derive aerosol optical thickness over land and ocean and estimate the type of the boundary layer aerosol mixture. The synergetic approach introduces new capabilities for operational aerosol retrieval from space, namely retrieval over land and differentiation of various aerosol types. Also important is the fact that it relies on an accurate cloud detection, which reduces erroneous aerosol detection significantly and enables the exploitation of partly cloud-covered spectrometer pixels.

[17] A first case study validation was performed with GOME cloud fractions up to 35%. This study showed good agreement of retrieved spectral aerosol optical thickness to ground-based sun photometer measurements with an error below 0.1 at 340–870 nm. This good spectral agreement indicates a good selection of the aerosol type. The derived aerosol type is also plausible for the region of the 14 validation stations (with two exceptions: one at Santa Cruz might be due to the low aerosol content of 0.12 in this pixel; and the one in Mongu could indicate difficulties with the dark field detection in this area, especially at this altitude of above 1000 m or limitations of aerosol retrieval in general for bright surfaces). It should be noted, however, that the aerosol optical thickness value at 550 nm (i.e., the total aerosol amount) has been correctly retrieved within the accuracy limits of the method for all 14 stations. Due to a very small number of exploitable ground measurements only 15 case studies (14 with ground-based and one airborne) could be performed so far. The validation of SYNAER results is rather difficult because it means comparing a point measurement from the AERONET sun photometers with an area averaged over $80 \times 40 \text{ km}^2$. However, the case study validation included pixels with a global distribution over a large part of the year, as well as several types of aerosols, and BLAOT values up to 0.68. So far, the validation focused on retrieval over land (which is one new capability of SYNAER). However, further validation efforts must include observations over ocean and a direct evaluation of the SYNAER selected mixture of aerosols by comparison with in situ observations. Especially, cases such as at Santa Cruz and Mongu must be looked at to define a more robust quality check of the retrieval results.

[18] Due to its experimental components, SYNAER requires further validation and optimization, which will be conducted with ENVISAT data. After future accounting for altitude dependency of the Rayleigh scattering especially in the UV by use of a digital elevation model validation sites

higher than 1500 m above sea level must be included. As varying chlorophyll concentration and consecutive absorption in the water are not taken into account, validation over ocean must assess the effects of this simplification. Additionally, the use of more validation measurements (AERONET, cross-sensor, cross-methodology) are planned to assess the accuracy of the retrieval of the basic aerosol components. By comparison to other complementary remote sensing aerosol measurements on the one hand an improvement of SYNAER as well as the other methods and on the other hand a better understanding of the global aerosols can be expected.

[19] Using GOME and ATSR-2 the spatial resolution (at least for the aerosol type retrieval from GOME pixels) is too coarse for detecting small-scale variabilities of the aerosol composition; however, the detection of local peaks in aerosol was demonstrated. With SCIAMACHY and AATSR a better spatial correlation (in the entire AATSR swath width of 512 km) with a slightly increased horizontal spectrometer resolution of $60 \times 30 \text{ km}^2$ will be available. SCIAMACHY has a wider spectral range (up to 2400 nm, GOME up to 790 nm), which will enable a better investigation of the aerosol type, especially for large particles, and the additional limb viewing geometry for stratospheric aerosol retrieval. Both instruments offer an improved data transmission rate and allow small SCIAMACHY pixels and orbitwise AATSR data throughout the entire mission. With swath widths of 960 km (GOME/SCIAMACHY) and 512 km (ATSR-2/AATSR), the data basis of SYNAER allows for global coverage about every 6 days. This means that from the satellite observations weekly products are feasible. In order to achieve daily synoptic maps data assimilation schemes will need to be developed - a new task that is currently being taken up by several groups in Europe. SYNAER results will be compared with the respective aerosol model results to eventually develop a suitable operational assimilation scheme for synoptic maps.

[20] Within the setup of a processor for atmospheric value added products, the German Remote Sensing Data Center (DFD) of the German Aerospace Center (DLR) will operationalize the SYNAER method for ENVISAT. The aim is to contribute a satellite based climatology of tropospheric aerosols for 10 years of ERS-2 and ENVISAT data (7/1995 to 6/2005) to improve the understanding of the global temporal-spatial distribution of aerosol loading and its major components. SYNAER could also be adapted to the sensor pair GOME-2/AVHRR, which will be flown for 15 years from 2005 on the 3 METOP platforms. Thus, potentially a 25-year data set can be derived with this method. One particular advantage of SYNAER is that it can be used to extract global aerosol information back to the year 1995. A direct implementation of the SYNAER resulting climatology data set in the global circulation model ECHAM [Röckner *et al.*, 1992] is under preparation since the SYNAER data set will follow the characteristics of the ground-based data set GADS (Global Aerosol Data Set) [Köpke *et al.*, 1997] which is currently under implementation in ECHAM. Thus, this data set may easily enable a more detailed treatment of aerosols in climate models. Furthermore, a direct comparison of the ground-based GADS and the satellite derived SYNAER climatologies is possible since both data sets rely on the same set of

representative aerosol components from the OPAC database.

[21] **Acknowledgments.** The results presented in this paper were achieved within the ESA-AO projects PAGODA (AO2.D107-1) and PAGODA-2 (AO3.218), through which the input data (GOME and ATSR-2) were acquired. The adaption of SYNAER to ENVISAT and production of an aerosol climatology will begin in the ESA-ENVISAT-AO project SENECA (AO ID-106). Our thanks go to Brent Holben/NASA-GSFC and the AERONET PIs for providing AERONET validation data and to our colleagues from the Institute for Atmospheric Physics, DLR, F. Petzold and A. Stifter, for the provision and evaluation of airborne LIDAR measurements in the Pfälzer Wald.

References

- Andreae, M. O., The dark side of aerosols, *Nature*, 409/410, 671, 2001.
- Charlson, R. J., and J. Heintzenberg (Eds.), *Dahlem Workshop Report on Aerosol Forcing of Climate*, 416 pp., John Wiley, New York, 1995.
- Holben, B. N., et al., AERONET: A federated instrument network and data archive for aerosol characterization, *Remote Sens. Environ.*, 66, 1–16, 1998.
- Holben, B. N., et al., An emerging ground-based aerosol climatology: Aerosol optical depth from AERONET, *J. Geophys. Res.*, 106, 12,067–12,097, 2001.
- Holzer-Popp, T., T. Kriebel, U. Böttger, M. Dameris, G. Gesell, T. König, R. Meerkötter, T. Rother, and M. Schroedter, PAGODA final report, *Schr. Dtsch. Fernerkundungsdatenzent. 1*, Dtsch. Zent. für Luft- und Raumfahrt, Oberpfaffenhofen, Germany, 1998.
- Holzer-Popp, T., and M. Schroedter, Retrieval of aerosol properties over land and ocean by exploiting the synergy of GOME and ATSR-2, paper presented at International Geoscience and Remote Sensing Symposium, Inst. of Electr. and Electron. Eng., Hamburg, Germany, 28 June to 2 July 1999.
- Holzer-Popp, T., M. Schroedter, and G. Gesell, High resolution aerosol maps exploiting the synergy of ATSR-2 and GOME, *Earth Obs. Q.*, 65, 19–24, 2000a.
- Holzer-Popp, T., M. Schroedter, G. Wendling, G. Gesell, C. Kiemle, A. Petzold, M. Fiebig, and A. Stifter, Synergetic retrieval of aerosol properties: from ERS to ENVISAT, paper presented at ERS-ENVISAT-Symposium, Eur. Space Agency, Gothenburg, Germany, 16–20 Oct. 2000b.
- Holzer-Popp, T., M. Schroedter, and G. Gesell, Retrieving aerosol optical depth and type in the boundary layer over land and ocean from simultaneous GOME spectrometer and ATSR-2 radiometer measurements, 1, Method description, *J. Geophys. Res.*, 107, doi:10.1029/2001JD002013, in press, 2002.
- Intergovernmental Panel on Climate Change (IPCC), *Climate Change: The 1990 and 1992 IPCC Assessments*, World Meteorol. Organ./U.N. Environ. Programme, June 1992.
- Intergovernmental Panel on Climate Change (IPCC), *Climate Change 1994*, Cambridge Univ. Press, New York, 1995.
- Jacobson, M. Z., Strong radiative heating due to the mixing state of black carbon in atmospheric aerosols, *Nature*, 409, 695–697, 2001.
- Köpke, P., M. Hess, I. Schult, and E. P. Shettle, Global aerosol data set, *Rep. 243*, Max-Planck-Inst. für Meteorol., Hamburg, Germany, 1997.
- Popp, T., Correcting atmospheric masking to retrieve the spectral albedo of land surfaces from satellite, *Int. J. Remote Sens.*, 16, 3483–3508, 1995.
- Popp, T., G. Gesell, T. König, T. Kriebel, R. Meerkötter, and H. Mannstein, Exploiting GOME and ATSR-2 data: First results of the PAGODA project, paper presented at 3rd ERS Symposium, Eur. Space Agency, Florence, Italy, 27–31 March 1997.
- Röckner, E., et al., Simulation of the present-day climate with the ECHAM model: Impact of model physics and resolution, *Rep. 93*, 171 pp., Max-Planck-Inst. für Meteorol., Hamburg, Germany, 1992.
- Tegen, I., A. A. Lacis, and I. Fung, The influence on climate forcing of mineral aerosols from disturbed soils, *Nature*, 380, 419–422, 1996.
- Vermote, E. F., N. El Saleous, C. O. Justice, Y. J. Kaufman, J. L. Privette, L. Remer, J. C. Roger, and D. Tanre, Atmospheric correction of visible to middle-infrared EOS-MODIS data over land surfaces: Background, operational algorithm and validation, *J. Geophys. Res.*, 102, 17,131–17,141, 1997.

G. Gesell, T. Holzer-Popp, and M. Schroedter, Deutsches Zentrum für Luft- und Raumfahrt E.V. (DLR), Deutsches Fernerkundungsdatenzentrum (DFD), Oberpfaffenhofen, D-82234 Wessling, Germany. (thomas.holzer-popp@dlr.de)

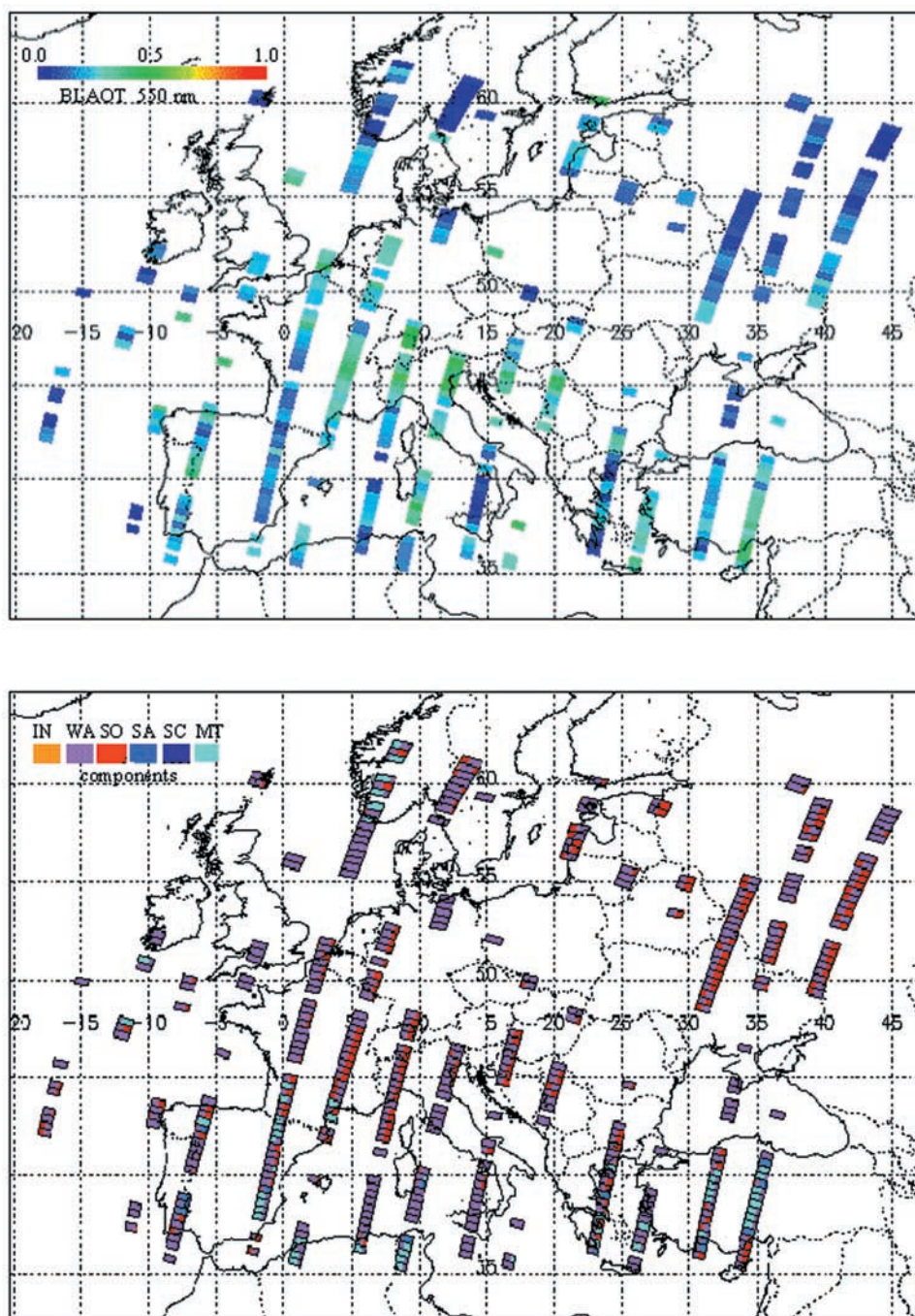


Figure 1. SYNAER 3-day map over Europe for 1–3 September 1995. Retrieved boundary layer optical thickness at 550 nm is shown in the upper part ranging from 0.03 to 0.55. Retrieved percentage contributions of six basic aerosol components (depicted as percentage of the pixel area) are shown in the bottom (IN, insoluble; WA, water-soluble; SO, soot; SA, sea salt accumulation mode; SC, sea salt coarse mode; MT, mineral transported). Cloud-covered GOME pixels above 50% cloud fraction are excluded. Pixels with large fit errors were excluded from both maps by the quality check. The ambiguity test was not applied.

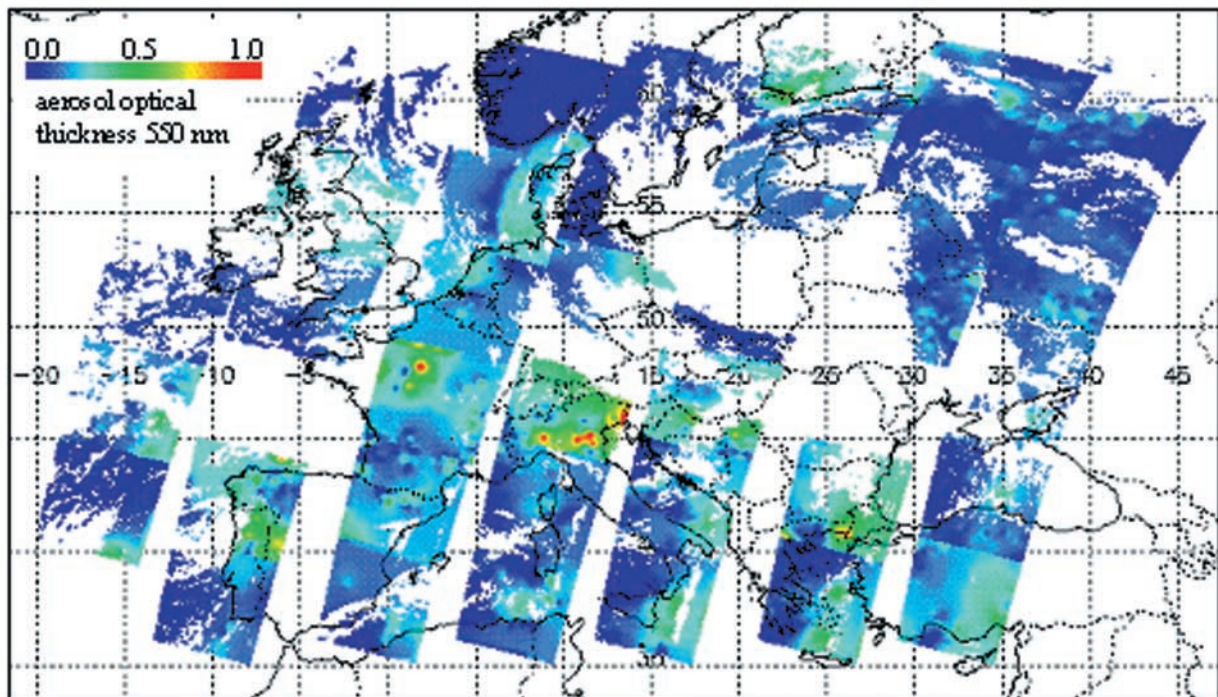


Figure 2. High-resolution aerosol map over Europe. Aerosol optical thickness at 550 nm for all daytime ATSR-2 frames acquired over Europe during the period 1–3 September 1995 (corresponding to the simultaneously measured GOME pixels in Figure 1) with a 1 km horizontal resolution. This result was achieved as post-processing of the SYNAER result based on GOME and ATSR-2 data shown in Figure 1. Cloud-covered pixels are left blank. Gaps between the 512 km swath of the ATSR-2 instrument are also left blank. Aerosol optical thickness ranges from 0.01 to 0.99.